JOC*Article*

Autoxidation of Hydrazones. Some New Insights

Maja Harej and Darko Dolenc*

University of Ljubljana, Faculty of Chemistry and Chemical Technology, Aškerčeva 5, SI-1000 Ljubljana, Slovenia

darko.dolenc@fkkt.uni-lj.si

Received May 23, 2007

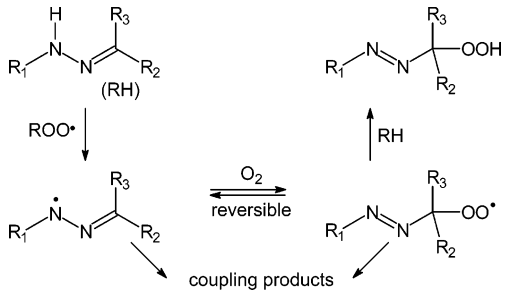

Autoxidation of hydrazones is a generally occurring reaction, leading mostly to the formation of α-azohydroperoxides. All structural kinds of hydrazones, having at least one hydrogen atom on nitrogen, are prone to autoxidation; however, there are marked differences in the rate of the reaction. Hydrazones of aliphatic ketones are 1−2 orders of magnitude more reactive than analogous derivatives of aromatic ketones. Even less reactive are the hydrazones of chalcones, which function also as efficient inhibitors of autoxidation of other hydrazones. These differences can be attributed to the reduction of the rate of the addition of oxygen to a hydrazonyl radical, which is a reversible reaction. In the case of conjugated ketones, it becomes endothermic, making this elementary step slow down and the chain termination reactions become important. Substituents influence the stability of hydrazonyl radicals and, consequently, the bond dissociation energies of the N−H bonds. In acetophenone phenylhydrazones, the substituents placed on the ring of hydrazine moiety exhibit a higher effect (Hammett $\rho = -2.8$) than those on the ketone moiety ($\rho = -0.82$), which denotes higher importance of the structure with spin density concentrated on nitrogen in delocalized hydrazonyl radical. Electronic effects of the substituents also affect the transition state for the abstraction of hydrogen atom by electrophilic peroxy radicals; NBO analysis display a negative charge transfer of about 0.4 eu from hydrazone to a peroxy radical in the transition state.

Introduction

Oxidation of materials with molecular oxygen is a ubiquitous process, important in living organisms, the environment, chemical technology, food processing, etc. Several excellent monographs and reviews address this topic, particularly the autoxidation of lipids and other biologically important materials.[1,2] Autoxidation of hydrazones is mostly neglected in these texts, despite the fact that the reaction is interesting also from a synthetic viewpoint. Primary products of the autoxidation, α-azo hydroperoxides, can be used as oxygen-transfer reagents[3] or reduced to α-azo alcohols, which serve as low temperature sources of various alkyl or aryl radicals,[4] as well as in other synthetic reactions.[5] Autoxidation of hydrazones is known for a long time and has been extensively investigated, especially

(1) (a) Denisov, E. T.; Afanas'ev, I. B. *Oxidation and Antioxidants in Organic Chemistry and Biology*; CRC Press: Boca Raton, 2005. (b) Denisov, E. T.; Sarkisov, O. M.; Likhtenshtein, G. I. *Chemical Kinetics. Fundamentals and New Developments*; Elsevier: Amsterdam, 2003. (c) Halliwell, B.; Guteridge, J. M. *Free Radicals in Biology and Medicine*; Oxford University Press: Oxford, 1999. (d) Akoh, C. C., Min, D. B., Eds. *Food Lipids*, 2nd ed.; Marcel Dekker: New York, 2002.

(2) Porter, N. A.; Caldwell, S. E.; Mills, K. A. *Lipids* **1995**, *30*, 277−290. Ingold, K. U.; Bowry, V. W.; Stocker, R.; Walling, C. *Proc. Natl. Acad. Sci. U.S.A.* **1993**, *90*, 45−49.

(3) Baumstark, A. L. *Bioorg. Chem.* **1986**, *14*, 326−343.

(4) Mathew, L.; Warkentin, J. *Can. J. Chem.* **1988**, *66*, 11−16. Chang, Y.-M.; Profetto, R.; Warkentin, J. *J. Am. Chem. Soc.* **1981**, *103*, 7189−7195. Jewel, D. R.; Mathew, L.; Warkentin, J. *Can. J. Chem.* **1987**, *65*, 311−315.

(5) Tezuka, T.; Sasaki, K.; Narita, N.; Fujita, M.; Ito, K.; Otsuka, T. *Tetrahedron Lett.* **1989**, *30*, 963−966. Baumstark, A. L.; Vasquez, P. C. *J. Org. Chem.* **1992**, *57*, 393−395.

10.1021/jo071091m CCC: $37.00
Published on Web 08/15/2007

in the first decades of the past century. In the 1970s, the interest in this process ceased, although many issues remained unresolved. Early researchers ascertained that the process takes place spontaneously, with no need for any external stimulus, such as light, although the irradiation may alter the rate of the reaction.[6] The reaction involves an addition of one molecule of oxygen to a hydrazone; however, the structure of the products was not clarified at that time.[7] It was found that the reactive hydrazones contain at least one hydrogen atom on nitrogen; i.e., they must be derived from primary hydrazines. Pausacker[8] and Criegee et al.[9] established that the products are α-azohydroperoxides, contrary to Busch and Dietz,[7] who proposed the formation of dioxetanes. The rate of the autoxidation of benzaldehyde phenylhydrazone was found to be influenced by solvent and substituents on either of the aromatic rings. Electron-donating substituents enhance the rate of autoxidation, whereas the electron-withdrawing ones diminish it. The effect is more pronounced by substituents placed on the hydrazine moiety rather than on aldehyde or ketone part of the hydrazone. According to these observations, a chain reaction was postulated, with the abstraction of hydrogen from NH group by peroxy radicals as the rate-determining step. Nonetheless, it was not clearly stated which hydrazones are prone to autoxidation and which are not.

In this paper, we present a systematic study of the reactivity of hydrazones toward molecular oxygen, with regard to their structure. The refined mechanism of the reaction is put forward, based on kinetic measurements and supported by quantum-chemical calculations.

Results and Discussion

The data obtained from previous literature are quite poor and insufficient to make any decisive conclusion about the crucial steps in the autoxidation process. Although Pausacker measured the reactivity of several benzaldehyde phenylhydrazones substituted on either ring, the published data are rather crude.[8] There were no measurements made on purely alkyl compounds or alkylhydrazones of aromatic ketones and vice versa. Therefore, we decided to measure the rate of autoxidation for a series of compounds to obtain additional or better data.

Kinetics. The rates of autoxidation were measured spectrophotometrically in heptane, saturated with oxygen under atmospheric pressure (98−100 kPa). Due to the high absorptivity of hydrazones and/or azohydroperoxides in the UV−vis, the concentration of hydrazone suitable for measurements was in the order of 1×10^{-4} M.[10] On the other hand, the concentration of oxygen in saturated solution in heptane at 20 °C was estimated to 13.0 mM,[11] thus enabling the pseudo first-order kinetics to be applied, which considerably simplifies the kinetic analysis.

The autoxidation of hydrazones is an autoinitiated reaction, with the initiation step not yet clarified. With the assumption

SCHEME 1

Initiation

$$RH + O_2 \xrightarrow{k_i} R^\bullet + HO_2^\bullet \quad (1)$$

Propagation

$$R^\bullet + O_2 \underset{k_{-1}}{\overset{k_1}{\rightleftharpoons}} RO_2^\bullet \quad (2)$$

$$RO_2^\bullet + RH \xrightarrow{k_2} RO_2H + R^\bullet \quad (3)$$

$$HO_2^\bullet + RH \xrightarrow{k_2} H_2O_2 + R^\bullet \quad (4)$$

$$2\,RO_2^\bullet \xrightarrow{k_3} 2\,RO^\bullet + O_2 \quad (5)$$

$$RO^\bullet + RH \xrightarrow{k_4} ROH + R^\bullet \quad (6)$$

Termination

$$2\,R^\bullet \xrightarrow{k_{t1}} RR \quad (7)$$

$$R^\bullet + RO_2^\bullet \xrightarrow{k_{t2}} RO_2R \quad (8)$$

$$2\,RO_2^\bullet \xrightarrow{k_{t3}} \text{molecular products} \quad (9)$$

that the initiation is a bimolecular reaction between the hydrazone and the O_2 molecule, Scheme 1 can be set up.

Taking into account that with the considerable chain length the rate of initiation equals the rate of termination, the following expression for the reaction rate can be derived (see the Supporting Information)

$$v = \frac{d[RO_2H]}{dt} = \frac{k_2 k_i^{1/2}[RH]^{3/2}[O_2]^{1/2}}{\left\{\frac{2k_{t1}}{K^2[O_2]^2} + \frac{2k_{t2}}{K[O_2]} + 2k_{t3}\right\}^{1/2}} \quad (10)$$

where $K = k_1/k_{-1}$.

When K and/or the concentration of O_2 are large, the terms containing k_{t1} and k_{t2} in the denominator can be ignored and the eq 10 is simplified.

$$\frac{d[RO_2H]}{dt} = -\frac{d[RH]}{dt} = k_2\sqrt{\frac{k_i}{2k_{t3}}}[RH]^{3/2}[O_2]^{1/2} = k_{obs}[RH]^{3/2}[O_2]^{1/2} \quad (11)$$

However, when this is not true, i.e., under the conditions of low concentration of oxygen or when the equilibrium (2) is lying on the reactant side, the omitted terms, which represent termination reactions, become significant. These reactions may shorten the chain length, thus reducing the overall rate of a chain reaction.

The factor $k_2(k_i/2k_{t3})^{1/2}$ is composed of rate constants of elementary steps the values of which are more or less unknown and can be replaced by k_{obs} (11). Integration at constant concentration of oxygen, i.e., under the conditions of first-order kinetics, then gives

$$[RH]^{-1/2} = [RH]_0^{-1/2} + \frac{k_{obs}}{2}[O_2]^{1/2}t \quad (12)$$

where $[RH]_0$ is the starting concentration of hydrazone.

(6) Stobbe, H.; Nowak, R. *Chem. Ber.* **1913**, *46*, 2887−2900.
(7) Busch, M.; Dietz, W. *Chem. Ber.* **1914**, *47*, 3277−3291.
(8) Pausacker, K. H. *J. Chem. Soc.* **1950**, 3478−3481.
(9) Criegee, R.; Lohaus, G. *Chem. Ber.* **1951**, *84*, 219−224.
(10) (a) Yao, H. C.; Resnick, P. *J. Org. Chem.* **1965**, *30*, 2832−2834. (b) Adembri, G.; Sarti-Fantoni, P.; Belgodere, E. *Tetrahedron* **1966**, *22*, 3149−3156.
(11) Reference 1a, p 33. Golovanov, I. B.; Zhenodarova, S. M. *Russ. J. General Chem.* **2005**, *75*, 1795−1797. Lühring, P.; Schumpe, A. *J. Chem. Eng. Data* **1989**, *34*, 250−252.

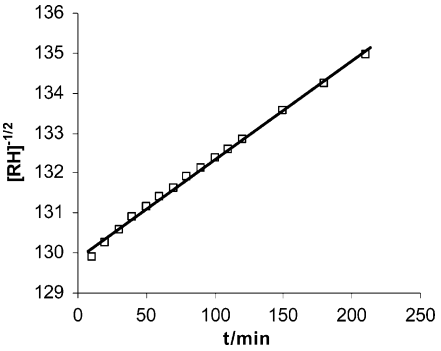

FIGURE 1. Plot of $[RH]^{-1/2}$ vs time for the autoxidation of **19** in heptane, saturated with oxygen at 20 °C.

TABLE 1. Rate Constants of the Autoxidation of Hydrazones[a]

hydrazone	$10^2 k_{obs}$ (M^{-1} s^{-1})	hydrazone	$10^2 k_{obs}$ (M^{-1} s^{-1})
5a	1.4	**14a**	8.4
6a	76	**15a**	0.74
7a	11×10^2	**16a**	0.23
8a	2.9×10^2	**17a**	0.016
8a[b]	2.8×10^2	**18a**	0.34
9a	1.0×10^2	**19a**	0.27
10a	7.6	**20a**	0.13
11a	0.87	**21a**	0.079
12a	0.11	**22a**	2.3×10^{-4}
13a	0.19		

[a] Measured spectrophotometrically as a decay of the absorbance of the starting hydrazone in heptane at 20.0 °C, saturated with O_2 (98−100 kPa). For relative errors, see the Supporting Information. [b] Measured in heptane saturated with air.

When measured $[RH]^{-1/2}$ were plotted against time, more or less linear plots were obtained (Figure 1), from which k_{obs} were determined. The measurements were not strictly reproducible; scattering of the rate constants up to 10% was usual, depending on hydrazone. Therefore, an average of two to four measurements is reported for each compound (Table 1). The purity of the hydrazone is crucial; traces of hydrazines or other impurities cause severe bending of the plot).

It can be clearly seen from Table 1 and Figure 1 that the rate of autoxidation is strongly influenced by the substituents at all three positions, R_1, R_2, and R_3 (Chart 1). Phenylhydrazones of aliphatic ketones **6a**−**10a** exhibit the highest reactivity, followed by purely aliphatic hydrazone **5a**, benzaldehyde alkylhydrazone **11a**, and arylhydrazones of aromatic ketones **12a**−**22a** as the least reactive. The electronic effect of substituents, placed on either of the aromatic rings of the hydrazone, is considerable; however, substituents on the ring in the hydrazine moiety exhibit a greater effect with $\rho = -2.3$ to -2.8 (acetone substituted-phenylhydrazones **6a**−**10a** and acetophenone substituted-phenylhydrazones **13a**−**17a**, respectively) compared to substituents on the ring in the ketone moiety, having $\rho = -0.82$ (Figure 2).[12] Rather high values of ρ indicate a substantial charge transfer in the transition state of a rate-determining step.

The effect of substituents on the rate can be interpreted by the influence of substituents on the energy of transition state in a rate-determining step, i.e., particularly step (3). In a chain reaction, there are several rate-determining steps represented by rate constants k_i, k_2, and k_t (eqs 10 and 11). Two of them, namely initiation and the abstraction of hydrogen in a propagation step, have most probably some common features.[13] Whatever the initiation reaction, it involves the formation of an initial hydrazonyl radical by the abstraction of the hydrogen atom from a hydrazone by a bi- or termolecular reaction of a hydrazone with molecular oxygen directly or indirectly via a redox process. Since the molecular oxygen is exceedingly electrophilic, a substantial charge transfer is expected to occur in the transition state. The same can be expected for the abstraction of a hydrogen atom in the propagation step by similarly electrophilic peroxy radicals.

The dependence of the rate on the concentration of oxygen is demonstrated by hydrazone **8a**, oxidized in heptane, saturated with pure oxygen or with air. The measured rate of oxidation in air is 2.2 times smaller than that in pure oxygen, yielding essentially the same value of the k_{obs} (Table 1).

Besides the initiation, one of the key rate-determining steps is the abstraction of the hydrogen atom from the hydrazone (10, 11). The rate is thus expected to be inversely proportional to the BDE N−H in the hydrazone, which is in turn linked to the stability of the hydrazonyl radical formed. To test this hypothesis, the energies of starting hydrazones, the corresponding hydrazonyl and azoperoxy radicals were calculated for a set of compounds (**1**−**13**, **18**−**22**). Compounds **1a**−**4a** were not synthesized and measured, but are model compounds, used for computational study only. Calculated reaction enthalpies are presented in Table 2.

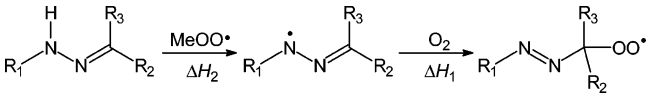

Enthalpies of the abstraction of hydrogen atom from hydrazones were calculated using one type of abstracting radical, namely MeO_2, for all substrates. In a real reaction, the abstracting radical is a peroxy radical, derived from a particular hydrazone (i.e., RO_2). In fact, the BDE O−H in various peroxides is hardly dependent on the type of R,[14,15] and the error thus made can be considered negligible.

The inspection of data presented in Table 2 reveals that the energetics of the abstraction of hydrogen atom from hydrazone is highly dependent on the number, type, and position of substituents in the molecule of the hydrazone. The methyl group at the hydrazine moiety (R_1, **2a**) lowers the energy of the abstraction by 14 kJ/mol (compared with **1a**). To the contrary, the methyl group placed at the ketone moiety (R_2, **3a**) gives rise to only 2.4 kJ/mol lowering of the BDE, and these effects are apparently quite additive. Replacement of an alkyl group at R_1 by aryl (**5a** → **6a**) causes additional lowering of the energy of the abstraction by 7.5 kJ/mol, which is reflected also in the rate of autoxidation. In a series of related acetone phenylhydrazones (**6a**−**10a**), the effect of the substituents placed on the

(12) The corresponding Hammett constants recalculated from from literature rates are −1.7 for benzaldehyde substituted-phenylhydrazones and approximately −0.7 for substituted-benzaldehyde phenylhydrazones.[8]

(13) Competition kinetics experiments with two hydrazones of similar type, e.g., two differently substituted acetophenone phenylhydrazones, measured by ^{1}H NMR exhibit the same reactivity patterns as in absolute kinetics. In this type of experiment, the differences in the rate of propagation should be reflected in the product ratios. Similar reactivities under each reaction condition point to a close relation between the initiation and propagation steps.

(14) Luo, Y.-R. *Handbook of Bond Dissociation Energies in Organic Compounds*; CRC Press: Boca Raton, 2003.

(15) Our calculations of BDE ROO-H (B3LYP/6-311G**) on several α-azohydroperoxides yielded values which differ up to 6 kJ/mol from each other.

CHART 1

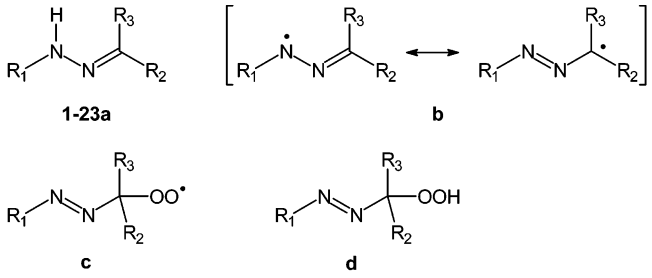

Compd	R_1	R_2	R_3	Compd	R_1	R_2	R_3
1	H	H	H	**13**	Ph	Ph	Me
2	Me	H	H	**14**	4-MeOPh	Ph	Me
3	H	Me	H	**15**	4-MePh	Ph	Me
4	Me	Me	H	**16**	4-ClPh	Ph	Me
5	c-hexyl	$-(CH_2)_5-$		**17**	4-CF_3Ph	Ph	Me
6	Ph	Me	Me	**18**	Ph	4-MeOPh	Me
7	4-MeOPh	Me	Me	**19**	Ph	4-MePh	Me
8	4-MePh	Me	Me	**20**	Ph	4-ClPh	Me
9	4-ClPh	Me	Me	**21**	Ph	4-CF_3Ph	Me
10	4-CF_3Ph	Me	Me	**22**	Ph	CH=CHPh	H
11	c-hexyl	Ph	H	**23**	4-MeOPh	CH=CHPh	H
12	Ph	Ph	H				

arylhydrazine ring can be observed. Electron-donating groups strongly reduce the N−H bond energies and the electron-withdrawing ones enhance them; the effect is reflected in the Hammett correlation (Figure 2) with an unusually high value of $\rho = -2.3$. A similar effect can also be seen in a series of related acetophenone substituted-phenylhydrazones (**13a**, **18a**−**21a**).

On the other hand, substitution of an alkyl group with aryl at the ketone moiety exhibits a smaller effect on the N−H bond

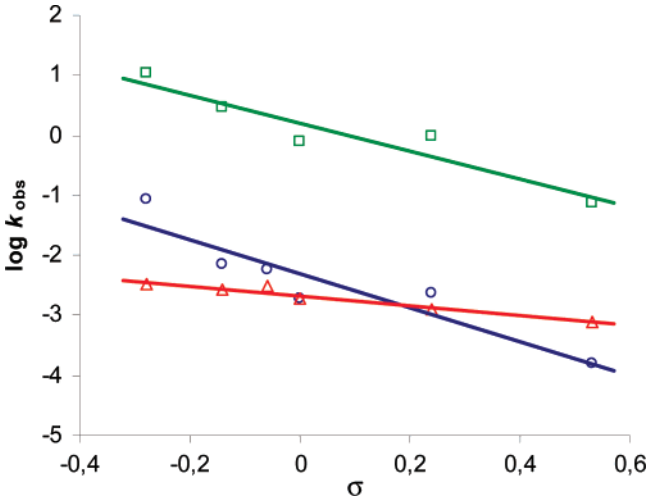

FIGURE 2. Hammett plots of the rates of autoxidation. □: acetone-substituted-phenylhydrazones, $\rho = -2.3 \pm 0.1$, $R^2 = 0.89$; ○: acetophenone substituted-phenylhydrazones, $\rho = -2.8 \pm 0.1$, $R^2 = 0.86$; △: substituted-acetophenone phenylhydrazones, $\rho = -0.82 \pm 0.1$, $R^2 = 0.95$.

TABLE 2. Calculated Reaction Enthalpies for the Abstraction of Hydrogen from a Hydrazone (ΔH_2) and the Addition of Oxygen to Hydrazonyl Radical (ΔH_1)[a]

hydrazone	ΔH_2[b] (kJ mol^{-1})	ΔH_1[c] (kJ mol^{-1})	hydrazone	ΔH_2 (kJ mol^{-1})	ΔH_1 (kJ mol^{-1})
1	26.5	−52.9	**10**	−10.1	−23.8
2	12.6	−62.9	**11**	−3.2	−25.4
3	24.1	−50.6	**12**	−10.1	0.5
4	8.7	−62.6	**13**	−28.9	3.7
5	−4.4	−57.6	**18**	−22.6	6.3
6	−11.9	−29.6	**19**	−20.0	3.7
7	−26.2	−28.2	**20**	−18.7	1.8
8	−16.2	−29.7	**21**	−15.5	2.8
9	−12.9	−26.6	**22**	−16.5	7.9

[a] Calculated at the B3LYP/6-311G** level as total enthalpies at 298K. [b] $H(R) + H(MeO_2H) - H(RH) - H(MeO_2)$. [c] $H(RO_2) - H(R) - H(O_2)$.

energy, and the same holds for the substituents on the arylketone ring as well. Nevertheless, aryl rings at the either side of the hydrazone hence stabilize the hydrazonyl radical and decrease the BDE of the N−H bond, but only the aromatic rings at the hydrazine moiety accelerate the autoxidation; however, those on the ketone moiety have the opposite effect.

The answer to this anomaly lies in the rightmost column (ΔH_1) of Table 2, presenting the enthalpies of the addition of oxygen to the hydrazonyl radical. These additions are known to be diffusion controlled and are generally exothermic in the beginning of the table, with a gradual decrease of the energy with increasing stabilization of the hydrazonyl radical. Introduction of an aryl ring at the position R_2 (**11**−**22**) sharply changes the sign of the enthalpy of the addition, which indicates that the addition of oxygen has become endothermic (Figure 3). The reason is the loss of conjugation of the hydrazonyl radical **b**

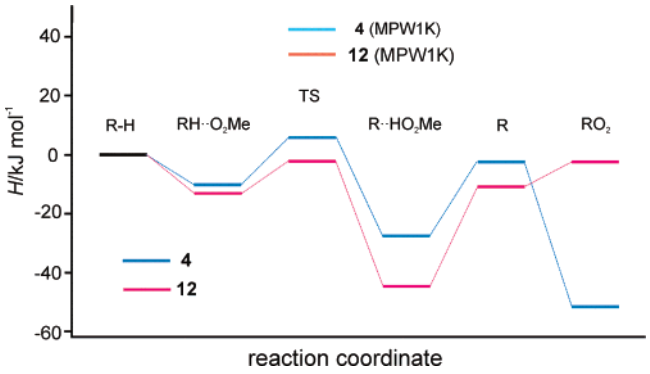

FIGURE 3. Energy diagram for the autoxidation of hydrazones **4a** and **12a**. *H* (kJ/mol) calculated at the B3LYP/6-311G** (for R and RO_2), B3LYP/6-311++G**, and MPW1K/6-311++G** (for RH··O_2-Me, TS and R··HO_2Me) levels.

SCHEME 2

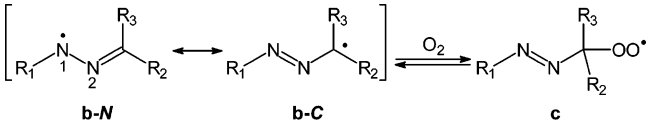

with the aromatic ring upon addition of the oxygen molecule (Scheme 2). In hydrazones of aliphatic ketones, there is no such stabilizing conjugation of the radical **b** with substituents R_2 or R_3 and the addition has smaller energetic effect. No appreciable activation barrier is expected for the attachment or detachment of an oxygen molecule, so this reaction step can be considered as a rapidly establishing equilibrium. The addition of oxygen molecule to delocalized C-centered radicals is, in some cases, known to be reversible, e.g., in the autoxidation of polyunsaturated fatty acids.[16]

The addition of an oxygen molecule to the radical **b** is an association reaction and in such case it is expected that entropic factors also play an important role. Calculated entropy change for the addition of oxygen molecule on radical **b** amounts to around −150 to −210 J mol^{-1} K^{-1}, which leads at 20 °C to approximately 44−60 kJ mol^{-1} on the ΔG scale.[17] This means that the addition of oxygen to hydrazonyl radical is no longer exothermic in ΔG terms but becomes nearly thermoneutral or slightly endothermic for hydrazones of aliphatic ketones (**1**−**10**) and substantially endothermic for hydrazones of aromatic ketones (**11**−**22**). The reaction (2) thus seems to be reversible with the equilibrium lying on the left side, at least for the hydrazones of the aromatic ketones, and it is becoming a slow step in the process. In such case the values of terms containing k_{t1} and k_{t2} (eq 10) increase, which results in a decrease of overall reaction rate. Along with the growing importance of termination reactions, one can expect an increase in the amount of the products thereof. ^{1}H NMR spectra of the reaction mixtures of autoxidation of hydrazones of aromatic ketones indeed display complex mixtures. As an example, in a spectrum of the reaction mixture of autoxidation of **18a** in acetone d_6, several peaks in the Me as well as in the OMe region can be found. In the aromatic region there is an abundance of unresolved multiplets between 6.6 and 8.0 ppm and in the OOH region two broad singlets appear with the integral of the major one of approx 0.35 of the expected value for pure hydroperoxide.

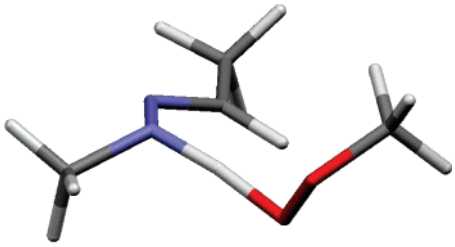

FIGURE 4. Transition state for the abstraction of a hydrogen atom by methylperoxy radical from **4a**, B3LYP/6-311++G**. Distances/Å: N−H 1.191; O−H 1.275. Angle/deg: N−H−O 172.

Hydrazones of conjugated aromatic aldehydes or ketones, e.g., cinnamaldehyde or benzalacetone, are even less reactive, despite the most exothermic abstraction of the hydrogen atom. Moreover, in mixtures with more reactive hydrazones they act as efficient autoxidation inhibitors. Autoxidation of cinnamaldehyde 4-methoxyphenylhydrazone (**23a**) at room temperature led in 6 days to the formation of a complex reaction mixture. ^{1}H NMR spectra exhibit at least five major peaks in the OMe region and very little OOH protons (few % of theoretical, 10.7 ppm in acetone-d_6). HPLC/MS analysis revealed a multitude of compounds, among which the majority exhibit a peak at the highest *m*/*z* at 534 which corresponds to the mass of a dimer + O_2 − 2. The isolation of products was not successful; however, analysis of the spectra led us to the conclusion that the compounds formed are most probably the coupling products of radicals R + RO_2.

The endothermicity of the addition of oxygen to the hydrazonyl radicals, derived from aromatic ketones and consequently, weakness of the C−OO(H) bond in the corresponding hydroperoxides is most probably the principal reason for the instability of the hydroperoxydes of this type.

As mentioned earlier, aromatic rings at R_1 and R_2 (or R_3) and the substituents placed on them, have different influences on the BDE of the N−H bond in hydrazone. NBO Analysis of the radical **1b** demonstrates the high spin density on N1 and N2 atoms (0.62 and 0.26, respectively), rather that on C (0.09), Scheme 2. The weight of the resonance structure **b-*N*** seems to be much higher than that of **b-*C*** and the substituent R_1 should have stronger effect on the energy than R_2 or R_3. Similarly, in radical **12b**, the spin density delocalized over aromatic ring at R_1 amounts to 0.27, which is more than twice of that on the aromatic ring at R_2 (0.13). These electronic effects are reflected in experimentally determined reactivities (Figure 2).

Reaction profiles for the series RH to $RO_2^\bullet$ exhibit a relatively low-lying transition state (B3LYP/6-311++G**, Figures 3 and 4), surrounded by two potential wells. One corresponds to a hydrogen-bonded complex of a molecule of hydrazone and peroxy radical (RH···O_2Me) before the transition state while the other represents a molecule of methyl hydroperoxide and hydrazonyl radical (R···HO_2Me) after the TS. Low activation enthalpy for the abstraction of hydrogen atom is consistent with smooth chain reaction with relatively long chains. The calculation of the activation enthalpy at the MPW1K/6-311++G** level, a method recommended for the transition states, yields substantially higher activation enthalpies (42 and 34 kJ mol^{-1}

(16) Tallman, K. A.; Pratt, D. A.; Porter, N. A. *J. Am. Chem. Soc.* **2001**, *123*, 11827−11828. Pratt, D. A.; Mills, J. H.; Porter, N. A. *J. Am. Chem. Soc.* **2003**, *125*, 5801−5810.

(17) Entropies for radicals of the type R and RO_2 for compounds **4** and **12** as well as O_2 calculated at the UB3LYP/6-311G** level were taken into account. Entropies are calculated for a gas-phase reaction; the effects in solution are presumably somewhat smaller.

for **4** and **12**, respectively).[18] Such high activation barriers would suggest slow reactions, which could not contribute to long chains in propagation step.[19] The values of activation enthalpies computed at the B3LYP level thus seem more realistic.

The most endothermic step in a series RH → RO_2 seems to be the dissociation of the R···HO_2R complex into R and HO_2R. However, this pathway can probably be avoided by the addition of molecular oxygen to the complex and dissociation of the new complex afterward. Such a "bypass" would considerably reduce the barrier going from R···HO_2R to RO_2 in the case of hydrazones of aliphatic ketones, such as **4**, but has no effect in the case of hydrazones of aromatic ketones (**12**).

NBO Analysis (B3LYP/6-311++G**) of the transition states displays a significant charge transfer between hydrazone and the methylperoxy radical in the transition state. The net charge on methylperoxy moiety is −0.442 and −0.381 for transition states **4 TS** and **12 TS**, respectively.

Conclusions

Hydrazones of all structural types, having at least one hydrogen atom on nitrogen, are susceptible to autoxidation, more reactive being the hydrazones of aliphatic ketones and those containing electron-donating groups, which lower the BDE of the N−H bond as well as the activation energy for the abstraction of hydrogen atom. This is evidenced by extensive charge transfer in the transition state, the electron density being shifted from hydrazone to electrophilic peroxy radical.

There are two types of hydrazones, in which the process is very slow. The first type contains strong electron-withdrawing groups which raise the BDE of the N−H bond the and also the activation barrier in the abstraction of the hydrogen atom, slowing down the rate of the abstraction of hydrogen atom (k_2, eq 3) and, consequently, the overall rate of the reaction.

The second type of slowly oxidizing compounds are hydrazones of aromatic ketones and conjugated vinylaromatic ketones (chalcones), which are even less reactive. In the autoxidation of these compounds a slow step is the addition of an oxygen molecule to the hydrazonyl radical, causing combination reactions to become important instead of the chain propagation. Autoxidation of such compounds does not yield α-azohydroperoxides as products, but rather complex reaction mixtures. Chalcone hydrazones are efficient autoxidation inhibitors for otherwise reactive hydrazones.

The high degree of negative charge transfer from hydrazone to peroxy radical in the transition state explains relatively high values of Hammett ρ values of substituents on the rate of the autoxidation.

Experimental Part

Theoretical Calculations. For DFT calculations, all structures were completely optimized at the B3LYP/6-311G** level for molecules and radicals and at the B3LYP/6-311++G** or MPW1K/6-311++G** for transition states and related structures. For radicals, analytical vibrational frequencies and enthalpies were calculated at the UDFT due to severe computation problems using restricted wavefunctions. On the other hand, appreciable spin contamination occurred using unrestricted DFT ($<S^2>$ was up to 0.785 for TS and 0.790 for radicals **b**) and for this reason, the geometries were reoptimized and total enthalpies were computed at RODFT at 298 K as follows: $H(R) = H(U) - E_{tot}(U) + E_{tot}(R)$. (Hydrazonyl and azoperoxy radicals have up to 10 kJ/mol lower energies when computed at UDFT.)[20] All computations were run on Jaguar, version 6.5, Schrodinger, LLC, New York, NY, 2005.

Synthesis. Caution! α-Azohydroperoxides are potentially explosive; however, we did not experience any accidents when working with these substances.

Hydrazones were synthesized in two ways: by Procedure 1, when hydrazine was used in its hydrochloride form (cyclohexanone cyclohexylhydrazone (**5a**),[21] acetone 4-methoxyphenylhydrazone (**7a**),[22] acetone 4-methylphenylhydrazone (**8a**),[23] acetone 4-chlorophenylhydrazone (**9a**),[22] benzaldehyde cyclohexylhydrazone (**11a**),[24] acetophenone 4-methoxyphenylhydrazone (**14a**),[25] acetophenone 4-methylphenylhydrazone (**15a**),[26] acetophenone 4-chlorophenylhydrazone (**16a**),[27] cinnamaldehyde 4-methoxyphenylhydrazone (**23a**)), or by procedure 2, when it was employed as a free base (acetone phenylhydrazone (**6a**),[28] acetone 4-trifluoromethylphenylhydrazone (**10a**), benzaldehyde phenylhydrazone (**12a**),[29] acetophenone phenylhydrazone (**13a**),[30] acetophenone 4-trifluoromethylphenylhydrazone (**17a**), 4-methoxyacetophenone phenylhydrazone (**18a**),[31] 4-methylacetophenone phenylhydrazone (**19a**),[32] 4-chloroacetophenone phenylhydrazone (**20a**),[33] 4-trifluoromethylacetophenone phenylhydrazone (**21a**), cinnamaldehyde phenylhydrazone (**22a**)).[34] NMR spectra were measured on a 300 MHz instrument and chemical shifts are reported relative to a $SiMe_4$ reference.

Procedure 1. To a suspension of 175 mg (1.00 mmol) of 4-methoxyphenylhydrazine hydrochloride and 120 μL (1.03 mmol) of acetophenone in 1 mL of ethanol purged with argon a solution of 84 mg (1.00 mmol) of sodium hydrogencarbonate in 1 mL of water was added dropwise while stirring. The reaction mixture was stirred at room temperature under argon for 2 h. It was then cooled to −30 °C, and the precipitate was filtered off and rinsed with water. The crystals thus obtained were recrystallized from petroleum ether yielding 194 mg of white crystals (**14a**, 81%): mp 113−114 °C (lit.[25] mp 115 °C).

Procedure 2. A 100 μL (1.016 mmol) portion of phenylhydrazine was dissolved in 0.5 mL of ethanol and purged with argon. 4-Methylacetophenone (136 μL, 1.019 mmol) was added to the solution, which was then left under argon at room temperature for 3 h. The mixture was cooled to −30 °C and the precipitate filtered off and rinsed with ethanol. The crude product was recrystallized from petroleum ether yielding 166 mg of white crystals (**19a**, 73%): mp 97−98 °C (lit.[32] mp 97 °C).

(18) Lynch, B. J.; Fast, P. L.; Harris, M.; Truhlar, D. G. *J. Phys. Chem. A* **2000**, *104*, 4811−4815.

(19) Rate constant calculated by Eyring equation, taking $\Delta H^{\ddagger} = 42$ kJ mol^{-1} and $\Delta S^{\ddagger} = 150$ J mol^{-1} K^{-1} as a typical value for a bimolecular reaction, is approximately 4×10^{-3} M^{-1} s^{-1}.

(20) Henry, D. J.; Parkinson, C. J.; Mayer, P. M.; Radom, L. *J. Phys. Chem. A* **2001**, *105*, 6750−6756.

(21) Sucrow, W.; Mentzel, C.; Slopianka, M. *Chem. Ber.* **1974**, *107*, 1318−1328.

(22) Chapman, N. B.; Clarke, K.; Hughes, H. *J. Chem. Soc.* **1965**, 1424−1428.

(23) Tsuge, O.; Kanemasa, S. *Bull. Chem. Soc. Jpn.* **1974**, *47*, 2676−2681.

(24) Busch, M.; Linsenmeier, K. *J. Prakt. Chem.* **1927**, *115*, 216−34.

(25) Suvorov, N. N.; Shkil'kova, V. N.; Podkhalyuzina, N. Ya. *Zh. Org. Khim.* **1983**, *19*, 2420−2423.

(26) Sah, P. P. T.; Lei, H.-H. *Science Repts. Natl. Tsing Hua Univ. [A]* **1933**, *2*, 1−5; *Chem. Abstr.* **1933**, *27*, 4222.

(27) Sah, P. P. T.; Lei, H.-H.; Shen, T. *Science Repts. Natl. Tsing Hua Univ. [A]* **1933**, *2*, 7−12; *Chem. Abstr.* **1933**, *27*, 4222.

(28) O'Connor, R. *J. Org. Chem.* **1961**, *26*, 4375−4380.

(29) Barnish, I. T.; Gibson, M. S. *J. Chem. Soc. C* **1970**, 854−859.

(30) Jarikote, D. V.; Deshmukh, R. R.; Rajagopal, R.; Lahoti, R. J.; Daniel, T.; Srinivasan, K. V. *Ultrason. Sonochem.* **2003**, *10*, 45−48.

(31) Skraup, S.; Guggenheimer, S. *Chem. Ber.* **1925**, *58B*, 2488−2500.

(32) Widman, O.; Bladin, J. A. *Chem. Ber.* **1886**, *19*, 583−589.

(33) Crowther, A. F.; Mann, F. G.; Purdie, D. *J. Chem. Soc.* **1943**, 58−68.

(34) Hearn, M. J.; Lebold, S. A.; Sinha, A.; Sy, K. *J. Org. Chem.* **1989**, *54*, 4188−4193.

Acetone 4-trifluoromethylphenylhydrazone (10a): procedure 2; brownish white crystals (from hexane); yield 68%; mp 44−45 °C; ^{1}H NMR ($CDCl_3$) δ 1.90 (s, 3H), 2.06 (s, 3H), 7.05 (s, 1H), 7.07 (d, J = 8.5 Hz, 2H), 7.46 (d, J = 8.5 Hz, 2H); ^{13}C NMR ($CDCl_3$) δ 15.5 (CH_3), 25.2 (CH_3), 112.2 (CH), 121.0 (q, $^2J_{F-C}$ = 32.5 Hz, C), 124.8 (q, $^1J_{F-C}$ = 271 Hz, CF_3), 126.5 (q, $^3J_{F-C}$ = 3.8 Hz, CH), 145.7 (C), 148.2 (C); IR (KBr, cm^{-1}) 3360 (w), 3312 (m), 2999 (w), 2948 (w), 2855 (w), 1618 (s), 1530 (s), 1410 (m), 1327 (br s), 1256 (s), 1155 (s), 1106 (br s), 1066 (s), 831 (s), 595 (m); UV (C_7H_{16}; λ_{max}/nm, (ϵ/L mol^{-1} cm^{-1})) 274.1 (3.52×10^4); MS (EI, 70 eV) *m*/*z* 216 (M$^+$, 100), 201 (13), 197 (15), 174 (18), 161 (44), 159 (43), 145 (14), 140 (29), 133 (9), 113 (10), 91 (7), 83 (8), 63 (8), 56 (53); HRMS (EI, 70 eV) calcd for $C_{10}H_{11}F_3N_2$ (M$^+$) 216.087433, found 216.088020 (Δ = 2.7 ppm). Anal. Calcd for $C_{10}H_{11}F_3N_2$ (216): C, 55.53; H, 5.13; N, 12.96. Found: C, 55.35; H, 4.83; N, 12.86.

Acetophenone 4-trifluoromethylphenylhydrazone (17a): procedure 2; white crystals (from petroleum ether); yield 61%; mp 105−106 °C; ^{1}H NMR ($CDCl_3$) δ 2.27 (s, 3H), 7.23 (d, J = 8.4 Hz, 2H), 7.32−7.42 (m, 3H), 7.51 (s, 1H), 7.52 (d, J = 8.4 Hz, 2H), 7.78 (dd, J = 8.3, 1.4 Hz, 2H); ^{13}C NMR ($CDCl_3$) δ 12.0 (CH_3), 112.7 (CH), 121.8 (q, $^2J_{F-C}$ = 32.3 Hz, C), 124.7 (q, $^1J_{F-C}$ = 269 Hz, CF_3), 125.7 (CH), 126.6 (q, $^3J_{F-C}$ = 3.8 Hz, CH), 128.40 (CH), 128.41 (CH), 138.7 (C), 143.0 (C), 147.7 (C); IR (KBr, cm^{-1}) 3357 (m), 3052 (w), 3040 (w), 2927 (w), 2851 (w), 1616 (s), 1528 (m), 1331 (br, s), 1264 (s), 1138 (s), 1107 (br, s), 1063 (s), 834 (s), 764 (s), 694 (m); UV (C_7H_{16}; λ_{max}/nm, (ϵ/L mol^{-1} cm^{-1})) 320.0 (2.11×10^4); MS (EI, 70 eV) *m*/*z* 278 (M$^+$, 100), 259 (7), 167 (5), 159 (7), 140 (6), 118 (55), 103 (8), 77 (69); HRMS (EI, 70 eV) calcd for $C_{15}H_{13}F_3N_2$ (M$^+$) 278.103083, found 278.103650 (Δ = 2.0 ppm). Anal. Calcd for $C_{15}H_{13}F_3N_2$ (278): C, 64.72; H, 4.71; N, 10.07. Found: C, 64.69; H, 4.79; N, 9.91.

4-Trifluoromethylacetophenone phenylhydrazone (21a): procedure 2; yellow crystals (from petroleum ether); yield 55%; mp 93−94 °C; ^{1}H NMR ($CDCl_3$) δ 2.23 (s, 3H), 6.91 (tt, J = 8.0, 1.3 Hz, 1H), 7.18 (dd, J = 8.0, 1.3 Hz, 2H), 7.30 (dt, J = 8.0, 1.3 Hz, 2H), 7.43 (s, 1H), 7.60 (d, J = 8.2 Hz, 2H), 7.89 (d, J = 8.2 Hz, 2H); ^{13}C NMR ($CDCl_3$) δ 11.6 (CH_3), 113.3 (CH), 120.7 (CH), 124.3 (q, $^1J_{F-C}$ = 272 Hz, CF_3), 125.2 (q, $^3J_{F-C}$ = 3.8 Hz, CH), 125.6 (CH), 129.3 (CH), 129.5 (q, $^2J_{F-C}$ = 32.4 Hz, C), 139.1 (C), 142.4 (C), 144.7 (C); IR (KBr, cm^{-1}) 3357 (m), 3056 (w), 2936 (w), 1603 (s), 1505 (s), 1409 (m), 1329 (s), 1248 (s), 1154 (s), 1115 (s), 1075 (s), 1012 (m), 841 (s), 750 (s), 692 (s), 507 (m); UV (C_7H_{16}; λ_{max}/nm, (ϵ/L mol^{-1} cm^{-1})) 336.0 (1.97×10^4); MS (EI, 70 eV) *m*/*z* 278 (M$^+$, 100), 263 (5), 259 (8), 186 (42), 145 (37), 92 (41), 69 (16), 65 (18), 57 (12); HRMS (EI, 70 eV) calcd for $C_{15}H_{13}F_3N_2$ (M$^+$) 278.103083, found 278.103820 (Δ = 2.6 ppm). Anal. Calcd for $C_{15}H_{13}F_3N_2$ (278): C, 64.72; H, 4.71; N, 10.07. Found: C, 64.37; H, 4.72; N, 9.82.

***trans*-3-Phenylprop-2-enal 4-methoxyphenylhydrazone (23a):** procedure 1; yellow crystals (from ethanol); yield 60%; mp 112−113 °C; ^{1}H NMR ($CDCl_3$) δ 3.75 (s, 3H), 6.60 (d, J = 16.0 Hz, 1H), 6.83 (dd, J = 6.8, 2.2 Hz, 2H), 6.95−7.03 (m, 3H), 7.20−7.25 (m, 1H), 7.29−7.7.34 (m, 2H), 7.40−7.45 (m, 4H); ^{13}C NMR ($CDCl_3$) δ 55.7 (CH_3), 114.0 (CH), 114.8 (CH), 126.0 (CH), 126.4 (CH), 127.8 (CH), 128.7 (CH), 133.4 (CH), 136.8 (C), 138.4 (C), 139.2 (CH), 153.9 (C); IR (KBr, cm^{-1}) 3298 (m), 3028 (w), 2994 (w), 2833 (m), 1616 (w), 1557 (m), 1514 (s), 1443 (m), 1242 (s), 1134 (s), 1097 (m), 1034 (m), 974 (s), 823 (s), 750 (s), 692 (s), 629 (m), 521 (m); UV (C_7H_{16}; λ_{max}/nm, (ϵ/L mol^{-1} cm^{-1})) 367.5 (3.06×10^4), 268.5 (1.23×10^4), 255.0 (1.24×10^4); MS (EI, 70 eV) *m*/*z* 252 (M$^+$, 76), 237 (6), 175 (6), 130 (9), 122 (100), 115 (5), 108 (8), 103 (10), 95 (12), 77 (15); HRMS (EI, 70 eV) calcd for $C_{16}H_{16}N_2O$ (M$^+$) 252.126263, found 252.127000 (Δ = 2.9 ppm). Anal. Calcd for $C_{16}H_{16}N_2O$ (252): C, 76.15; H, 6.40; N, 11.11. Found: C, 75.90; H, 6.49; N, 11.05.

Autoxidation. Autoxidation of the hydrazones of aliphatic ketones led mainly to α-azohydroperoxides, while those of aromatic carbonyl compounds gave complex mixtures. Unfortunately, we were unable to isolate the products in pure form due to their instability. Some compounds crystallized from the reaction mixture in hexane upon cooling, but decomposed into a brown oil during the filtration. The identity of the products was assigned on the basis of their ^{1}H and ^{13}C NMR spectra. Hydroperoxydes **5d**,[35] **11d**,[24] **12d**,[10a] **13d**,[36] **16d**,[36] and **18d**[37] are known compounds.

Typical Procedure. A 40 mg (0.246 mmol) portion of acetone 4-methylphenylhydrazone was dissolved in 0.7 mL of acetone-d_6 (Aldrich, 99.9% D, water content approximately 0.04%) or benzene-d_6 (Euriso-top 99.6% D, H_2O < 0,02%) and purged with oxygen at intervals. The course of reaction was followed by thin layer chromatography (silica, 2:1 dichloromethane hexane). In 4 h, the starting hydrazone was completely converted into 2-(4-methylphenylazo)propane-2-hydroperoxide **8d**.

The following hydroperoxides were not isolated; their spectra were measured in the reaction mixtures in NMR solvents acetone-d_6 or benzene-d_6. Hydroperoxides **15d**, **17d**, and **19d**−**22d** were not formed pure enough to allow their spectra to be interpreted unabiguously.

2-Phenylazopropane 2-hydroperoxide (6d): ^{1}H NMR (acetone-d_6) δ 1.44 (s, 6H), 7.51−7.53 (m, 3H), 7.74−7.77 (m, 2H), 10.81 (s, 1H); ^{13}C NMR (acetone-d_6) δ 23.0 (CH_3), 104.7 (C), 124.1 (CH), 130.9 (CH), 132.8 (CH), 153.6 (C); IR (NaCl, cm^{-1}) 3399 (br, m), 3068 (w), 2994 (m), 2942 (m), 1596 (w), 1527 (m), 1455 (s), 1361 (s), 1177 (s), 1147 (s), 844 (m), 765 (s), 690 (s); UV (C_7H_{16}; λ_{max}/nm, (ϵ/L mol^{-1} cm^{-1})) 265.9 (1.07×10^4), 411.0 (135).

2-(4-Methoxylphenylazo)propane 2-hydroperoxide (7d): ^{1}H NMR (acetone-d_6) δ 1.41 (s, 6H), 3.88 (s, 3H), 7.05 (dd, J = 6.9, 2.2 Hz, 2H), 7.76 (dd, J = 6.9, 2.2 Hz, 2H), 10.73 (s, 1H); ^{13}C NMR (acetone-d_6) δ 23.1 (CH_3), 57.0 (CH_3), 104.3 (C), 115.9 (CH), 126.0 (CH), 147.6 (C), 164.0 (C); IR (NaCl, cm^{-1}) 3404 (br, m), 2993 (m), 2940 (m), 2840 (w), 1603 (m), 1520 (s), 1254 (s), 1177 (m), 1142 (s), 1030 (m), 838 (m); UV (C_7H_{16}; λ_{max}/nm, (ϵ/L mol^{-1} cm^{-1})) 303.0 (8.52×10^3), 402.5 (131).

2-(4-Methylphenylazo)propane 2-hydroperoxide (8d): ^{1}H NMR (acetone-d_6) δ 1.42 (s, 6H), 2.39 (s, 3H), 7.33 (dd, J = 6.4, 1.7 Hz, 2H), 7.66 (dd, J = 6.4, 1.7 Hz, 2H), 10.77 (s, 1H); ^{13}C NMR (acetone-d_6) δ 22.3 (CH_3), 23.1 (CH_3), 104.5 (C), 124.2 (CH), 131.4 (CH), 143.2 (C), 151.6 (C); IR (NaCl, cm^{-1}) 3399 (br, m), 2992 (m), 2940 (m), 1604 (m), 1526 (s), 1360 (s), 1179 (s), 1148 (s), 824 (s); UV (C_7H_{16}; λ_{max}/nm, (ϵ/L mol^{-1} cm^{-1})) 276.6 (9.25×10^3), 408.5 (136).

2-(4-Chlorophenylazo)propane 2-hydroperoxide (9d): ^{1}H NMR (acetone-d_6) δ 1.43 (s, 6H), 7.56 (dd, J = 6.8, 2.2 Hz, 2H), 7.77 (dd, J = 6.8, 2.2 Hz, 2H), 10.84 (s, 1H); ^{13}C NMR (acetone-d_6) δ 23.0 (CH_3), 104.8 (C), 125.8 (CH), 131.1 (CH), 138.2 (C), 152.1 (C); IR (NaCl, cm^{-1}) 3399 (br, m), 2993 (m), 2940 (m), 2865 (w), 1583 (m), 1524 (s), 1477 (s), 1361 (s), 1175 (s), 1147 (m), 1087 (s), 1009 (m), 836 (s); UV (C_7H_{16}; λ_{max}/nm, (ϵ/L mol^{-1} cm^{-1})) 275.5 (9.54×10^3), 411.4 (118).

2-(4-Trifluoromethylphenylazo)propane 2-hydroperoxide (10d): ^{1}H NMR (acetone-d_6) δ 1.46 (s, 6H), 7.88−7.94 (m, 4H), 10.91 (s, 1H); ^{13}C NMR (acetone-d_6) δ 23.0 (CH_3), 105.2 (C), 124.7 (CH), 126.0 (q, $^1J_{F-C}$ = 272 Hz, CF_3), 128.3 (q, $^3J_{F-C}$ = 3.9 Hz, CH), 133.6 (q, $^2J_{F-C}$ = 32.3 Hz, C), 155.7 (C); IR (NaCl, cm^{-1}) 3397 (br, m), 2998 (m), 2944 (w), 1615 (m), 1414 (m), 1326 (s), 1171 (s), 1131 (s), 1066 (s), 849 (m), 658 (m); UV (C_7H_{16}; λ_{max}/nm, (ϵ/L mol^{-1} cm^{-1})) 259.0 (9.87×10^3), 412.5 (162).

1-Phenylazo-1-(4-methoxyphenyl)ethyl 1-hydroperoxide (14d): ^{1}H NMR (C_6D_6) δ 1.89 (s, 3H), 3.17 (s, 3H), 6.64 (dd, J = 6.9, 2.2 Hz, 2H), 7.06 (tt, J = 7.6, 1.5 Hz, 1H), 7.15 (dt, J = 7.6, 1.5 Hz, 2H), 7.63 (dd, J = 6.9, 2.2 Hz, 2H), 7.71 (dd, J = 7.6, 1.5 Hz, 2H), 9.73 (s, 1H); ^{13}C NMR (C_6D_6) δ 23.7 (CH_3), 55.0 (CH_3), 104.5 (C), 114.4 (CH), 125.1 (CH), 127.2 (CH), 128.5 (CH), 128.6 (CH),

(35) Hawkins, E. G. E. *J. Chem. Soc. C* **1971**, 1474−1477.
(36) Tezuka, T.; Ando, S. *Chem. Lett.* **1986**, 1671−1674.
(37) Baumstark, A. L.; Vasquez, P. C. *J. Phys. Org. Chem.* **1988**, *1*, 259−265.

140.5 (C), 145.7 (C), 162.7 (C); IR (NaCl, cm^{-1}) 3381 (br, m), 3062 (w), 3002 (m), 2940 (w), 2839 (m), 1675 (m), 1601 (s), 1514 (s), 1447 (m), 1363 (m), 1313 (m), 1252 (s), 1106 (m), 1026 (s), 838 (s), 760 (s), 696 (s).

UV Kinetics. Rates of autoxidation of the hydrazones of aromatic ketones were measured as a decay of absorbance of the hydrazone UV band at 320−360 nm. In the case of aliphatic arylhydrazones, absorption maxima of hydrazones are partially overlapped with those of hydroperoxides (around 260 nm). In these cases, absorbance of product hydroperoxide (around 410 nm) was also monitored but both measurements yielded essentially the same result.

Typical Procedure. A 0.20 mg (8.92×10^{-4} mmol) portion of acetophenone 4-methylphenylhydrazone (**15a**) was dissolved in 0.5 mL of heptane (Riedel-de Haen, $H_2O < 0.01\%$) purged with argon. A 100 μL portion of the solution was injected into a cuvette containing 3 mL of heptane purged with oxygen, yielding the hydrazone concentration of 5.94×10^{-5} mol L^{-1}. A spectrum in the range 500−230 nm was scanned at 10 min intervals until the reaction time reached 3.5 h. Absorbance values at λ_{max} 328 nm were used for computations.

Acknowledgment. We thank the Slovenian Research Agency for financial support, Drs. Bogdan Kralj and Dušan Žigon for mass spectra, Dr. Drago Kočar for HPLC/MS analyses, and Dr. Črtomir Podlipnik and Profs. Božo Plesničar and Andrej Jamnik for helpful discussions.

Supporting Information Available: Derivation of kinetic expressions, rate constants of the autoxidation of hydrazones (with errors), computed thermochemical data, and Cartesian coordinates of the hydrazones, hydrazonyl and α-azoperoxy radicals, and some transition states. ^1H and ^{13}C NMR spectra of compounds **10a**, **17a**, **21a**, **23a**, **6d**−**10d**, and **14d**. This material is available free of charge via the Internet at http://pubs.acs.org.

JO071091M